Additional Formation of Brønsted Acid Sites on Silica-Alumina Catalyst Surfaces by Depositing Silica Component

Satoshi SATO,* Masahiro HIRATSUKA, Toshiaki SODESAWA, and Fumio NOZAKI
Department of Applied Chemistry, Faculty of Engineering, Chiba University,
Yayoi-cho, Chiba 260

(Received January 21, 1991)

The chemical vapor deposition (CVD) of silica onto an amorphous silica–alumina was investigated using tetraethoxysilane in order to create Brønsted acid sites on the surface of original silica–alumina. Silica loading could be readily controlled by the CVD time at 160 °C; the silica covered an internal wall of mesopore of the support of silica–alumina. The resulting CVD silica–alumina was catalytically more active than the original silica–alumina support for such test reactions as the cracking of cumene and the isomerization of 1-butene. The characteristic changes in the amount of Brønsted acid sites were clarified by means of the temperature-programmed desorption of adsorbed 2,6-dimethylpyridine. Strong Lewis acid sites of the original silica–alumina were converted into strong Brønsted acid sites upon depositing the silica component.

Chemical vapor deposition (CVD) techniques are effective for attaining the high dispersion of a deposit on the surface of a catalyst support, and have recently been investigated regarding both the modification and preparation of solid acid catalysts.[1-9] We previously reported a supported type of silica–alumina catalyst prepared by depositing silica on an alumina surface.[5,9] Silica was effectively deposited onto the alumina by using tetraethoxysilane at 240 °C in the presence of oxygen; silica loading was readily controlled by the deposition time. The obtained alumina-supported silica catalyst was found to have predominantly Brønsted acid sites which are transformed from the Lewis acid sites of an alumina surface. The silica–alumina catalyst exhibited catalytic activities for several reactions such as cracking, isomerization, and dehydration.

Silica–alumina is an important catalyst for manufacturing various petrochemical products, and is commercially prepared by wet methods, such as co-precipitation and co-gelation. Although the conventional preparation methods are suitable for obtaining a "bulk" level dispersion of the binary oxide component, the respective oxide species do not disperse atomically. Thus, amorphous silica–alumina usually has both Brønsted and Lewis acid sites. In contrast to the wet methods, CVD techniques are attractive for surface modifications used to attain atomical dispersions of other oxide species on the surface of a catalyst support.

If the Lewis acid sites of amorphous silica–alumina are able to be converted into Brønsted acid sites by the deposition of silica, the catalytic properties must be improved. In this paper we describe various experimental results concerning the CVD of silica onto an amorphous silica–alumina support commercially produced by the co-gelation preparation method. In addition, we describe the acidic character of the CVD silica–alumina catalyst, which has been clarified by means of temperature-programmed desorption (TPD) using 2,6-dimethylpyridine as an adsorbate, together with the pore characteristics.

Experimental

Commercial silica–alumina (N631-L) with a specific surface area of 420 $m^2\ g^{-1}$, an alumina content of 13 wt%, and a granule size of 24—60 mesh was supplied by Nikki Chemical Co., Ltd. A CVD silica–alumina catalyst was prepared at the prescribed temperatures by bringing tetraethoxysilane vapor together with a carrier gas into contact with the silica–alumina support in a CVD reactor made up of a Pyrex glass tube rotating in an electrical furnace inclined at 45°;[9] the flow rates of tetraethoxysilane and the carrier gas were 2.7 and 400 mmol h^{-1}, respectively. After CVD operation, the sample was calcined at 550 °C for 3 h in an air atmosphere. The silica loading was calculated by measuring the weight increase of the CVD samples after calcination.

The cracking of cumene was tested at 350 °C using a fixed-bed continuous-flow apparatus under atmospheric pressure at a W/F of 28 g h mol^{-1}, where W is the weight of the catalyst and F is the molar flow rate of cumene, together with a nitrogen carrier gas (15 ml min^{-1}). The reactor effluent was analyzed by on-line GLC using a column of Bentone 34 and dinonyl phthalate (1 m).

The isomerization of 1-butene was performed in a closed circulation reactor comprising a circulation volume of 200 ml. After a catalyst (55 mg) had been evacuated at 200 °C for 1 h, the reaction was carried out at 50 °C at an initial pressure of 22 kPa. The products were analyzed by on-line GLC with a VZ-7 column (4.5 m). The isomerization activity was evaluated by the first-order rate constant during the initial reaction period.

A BET surface area and pore characteristics were obtained by nitrogen physisorption at −196 °C. The pore volume distribution was calculated using the method of Cranston and Inkley[10] and the desorption isotherm of nitrogen. A T-plot, giving an information about micropores with radii less than 0.35 nm, was also obtained from the desorption isotherm according to the articles by Boer and co-workers.[11-13]

A TPD measurement of the adsorbed pyridine or 2,6-dimethylpyridine was performed in order to evaluate the acidic property. After a sample (10 mg) had been evacuated at 500 °C for 1 h, pyridine was injected at 200 °C; the sample was then evacuated at 200 °C for 1 h. The TPD measurement was run from 200 to 700 °C at a heating rate of 5 °C min^{-1}. The desorbed pyridine was bubbled into a conductivity cell containing 0.5 mmol dm^{-3} of a sulfuric acid solution (30.0 g) together with nitrogen flow (70 ml min^{-1}); the amount of desorbed pyridine was monitored by the change in the solution conductivity.[14] The obtained cumulative curve differentiates to give an acid strength distribution as a function of desorption temperature.

Results and Discussion

Catalyst Preparation. Figure 1 shows the influence of the CVD temperature and time upon silica loading. In a stream of air, silica loading was increased with the CVD temperature at temperatures below 200 °C, and maximized at nearly 200 °C. Above this temperature, the silica loading decreased with the CVD temperature; above 280 °C the obtained catalyst had a color which varied from brown to black, due to coking. Thus, the optimum CVD temperature was found to be below 200 °C. At CVD temperature of 160 °C, the silica loading increased monotonously with the CVD time up to 2 h, and then leveled off. The silica loadings were 0.20 and 0.39 g/g-support for 2 and 8 h, respectively. In a stream of nitrogen, the silica loading also changed with the CVD time at 160 °C in the same manner as in the presence of oxygen. It can consequently be said that silica loading is readily controlled by the CVD time at 160 °C. No oxygen was needed for to accelerate the deposition rate at 160 °C, although oxygen was effective for the acceleration of silica deposition onto an alumina support at 240 °C.[9] Silica deposition onto silica–alumina occurred at lower temperatures (about 80 degree) compared to that for silica deposition onto an alumina support. In a stream of nitrogen above 200 °C, silica loading was almost unchanged with the CVD temperature, whereas it varied with the CVD temperature below 200 °C in a similar way as in air. This observation is presumed to be related to the deposition rate, as will be discussed later.

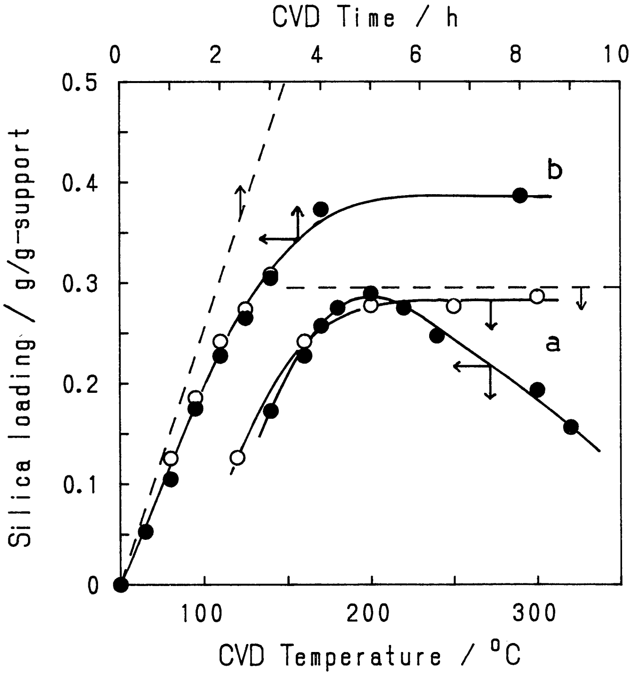

Fig. 1. Effect of CVD temperature and time. a, CVD was operated for 2 h; b, CVD was operated at 160 °C; ●, CVD was operated in air; ○, in nitrogen. Dashed line denotes the critical deposition amount limited by an amount of fed tetraethoxysilane.

Physical Properties. Changes in the surface area of CVD catalysts with silica loading are shown in Fig. 2. For CVD catalysts prepared at 160 °C, the surface area (based on the unit weight of the original silica–alumina support) slightly decreased with an increase in silica loading up to a loading of 0.2 g/g-support; it then decreased steeply. For an alumina support which has relatively large mesopores (ranging from 4 to 20 nm in diameter[9]), the deposited silica is uniformly dispersed on the support, since the surface area (based on the unit weight of the support) is almost unchanged, irrespective of the silica loading. For the present silica-alumina, the deposition of silica is considered to be affected by the pore structure of the support. Figure 3 shows the pore volume distribution of CVD catalysts together with the original silica–alumina support. The silica–alumina support had 0.47 ml g^{-1} of total pore volume and a maximum pore volume at a diameter of about 3.8 nm, which was smaller than that of the alumina support mentioned above. The CVD catalysts had the maximum pore volume at a diameter close to 3.8 nm, although the total pore volume was significantly decreased with silica loading. Furthermore, for CVD catalysts prepared at

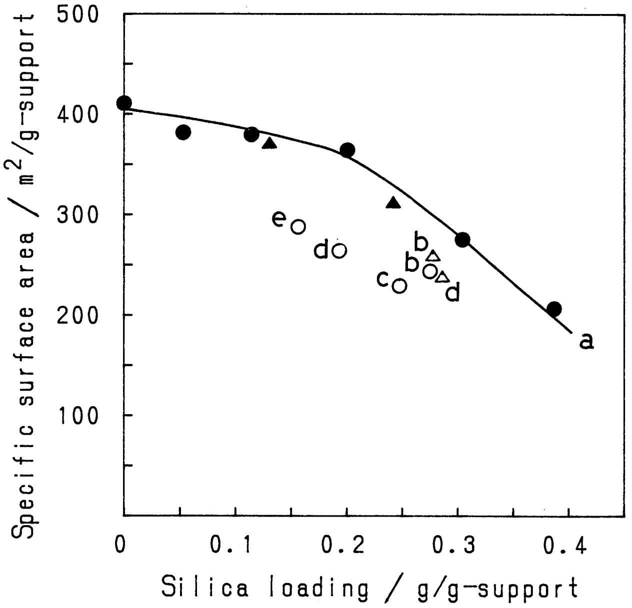

Fig. 2. Change in the surface area of a CVD catalyst with silica loading. ●, ○, CVD was operated in air; ▲, △, in nitrogen. a (solid line), prepared at 160 °C; b, 200 °C; c, 240 °C; d, 300 °C; e, 320 °C,

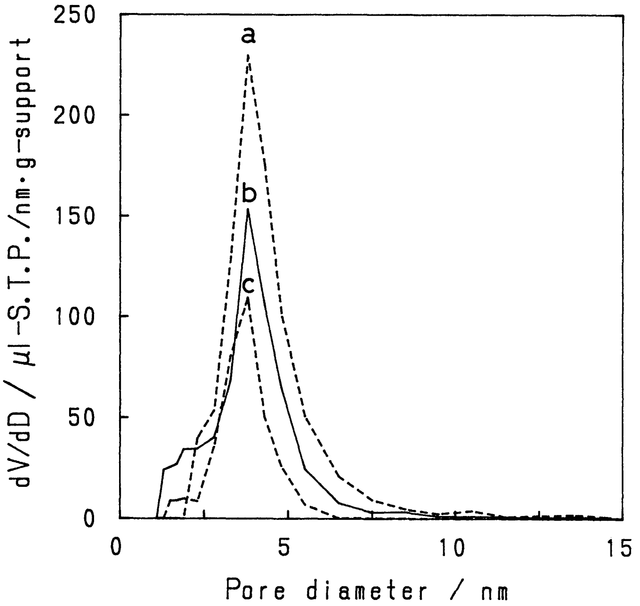

Fig. 3. Pore volume distribution of CVD catalysts. a, Original silica–alumina support; b, CVD catalyst (silica loading, 0.20 g/g-support); c, CVD catalyst (silica loading, 0.39 g/g-support).

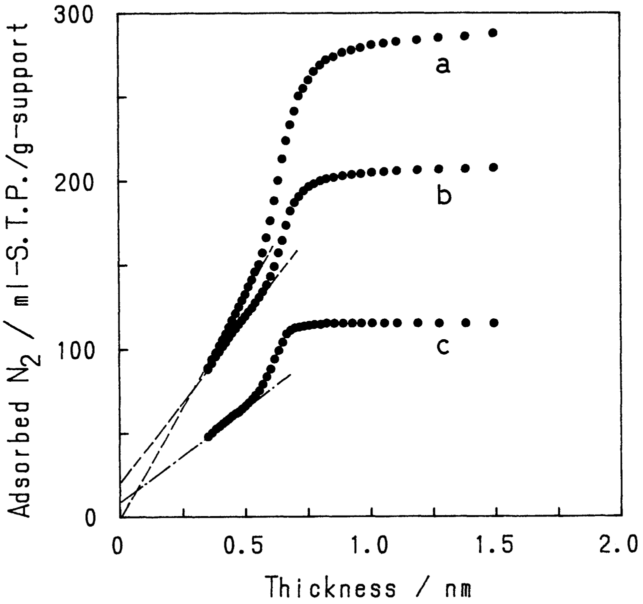

Fig. 4. T-plot for CVD catalysts. Symbols as those in Fig. 3.

temperatures higher than 200 °C in air, the surface area was much smaller than those prepared at 160 °C (Fig. 2). This indicates that aggregated deposition occurred in the neighborhood of the entrance of the micropores of the support; it then followed by the closure of the micropores at higher temperatures in air owing to a too-fast deposition. For a catalyst prepared at 300 °C in nitrogen, however, the surface area was not so small as those prepared in air. Since oxygen results in an aggregated deposition of silica at high temperatures (above 200 °C), the surface area steeply decreased.

In order to elucidate the existence of micropores under a diameter of 0.7 nm, a T-plot was examined according to the procedure proposed by Boer et al.[11–13] T-plots for CVD catalysts are shown in Fig. 4. A T-plot passes through the origin for a sample having no micropores, whereas it has an intercept which expresses the micropore volume for a sample having micropores.[13] Thus, an original silica–alumina support has no micropores because of the passing through the origin in the T-plot. For a CVD catalyst with a silica loading of 0.20 g/g-support, micropores (21 ml-STP) were generated with a small decrease in the BET surface area (Fig. 4b). Further silica deposition (0.39 g/g-support) led to a decrease in the micropore volume (10 ml-STP) together with a large decrease in the surface area (Figs. 2 and 4c). The deposition of silica resulted in the formation of micropores in the silica–alumina support. These results indicate that silica deposition develops on the interior wall of mesopore in such a characteristic way that the pore size decreases with silica deposition.

Acidic Properties. It has been known that 2,6-dimethylpyridine (2,6-DMP) selectively adsorbs on Brønsted acid sites, but not on Lewis acid sites because of a steric hindrance of two methyl groups, whereas sterically nonhindered pyridine adsorbs on both Brønsted and Lewis acid sites.[15,16] 2,6-DMP has been used for the characterization of acid surfaces with pulse adsorption,[15] IR spectroscopy,[16] and gravimetric titration.[17] We recently applied the TPD measurement of adsorbed 2,6-DMP to the elucidation of the acidic nature of an alumina-supported silica catalyst.[14] This investigation has elucidated that silica deposition creates Brønsted acid sites on the surface of alumina together with the disappearance of Lewis acid sites.

The TPD spectra of adsorbed pyridine and 2,6-DMP are illustrated in Fig. 5. The original silica–alumina support had a large desorption peak of pyridine and a somewhat smaller peak of 2,6-DMP than that of pyridine at peak tops of about 300 °C. Since curve b shows the acid strength distribution of Brønsted acid sites, the difference between curves a and b is a measure of Lewis acid sites. The silica–alumina support dominates Brønsted acid sites with a small amount of Lewis acid sites. This fact is also supported by the ^{31}P NMR of trimethylphosphine adsorbed on it.[9] In contrast, for a CVD catalyst loaded 0.20 g/g-support of silica, it had no significant difference between two distribution curves of pyridine and 2,6-DMP. This indicates that the CVD catalyst has dominantly Brønsted acid sites. In addition, the total numbers of acid sites, represented by the amount of desorbed pyridine, were reduced, as can be seen from a comparison of curves c and a. Moreover, the amount of desorbed 2,6-DMP decreased in the low-

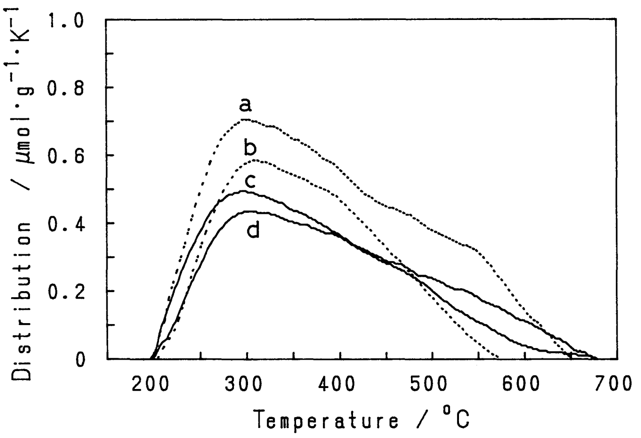

Fig. 5. TPD profiles of adsorbed pyridine and 2,6-dimethylpyridine. Original silica–alumina support (dotted line): a, pyridine; b, 2,6-DMP; CVD catalyst (silica loading, 0.20 g/g-support): c, pyridine; d, 2,6-DMP.

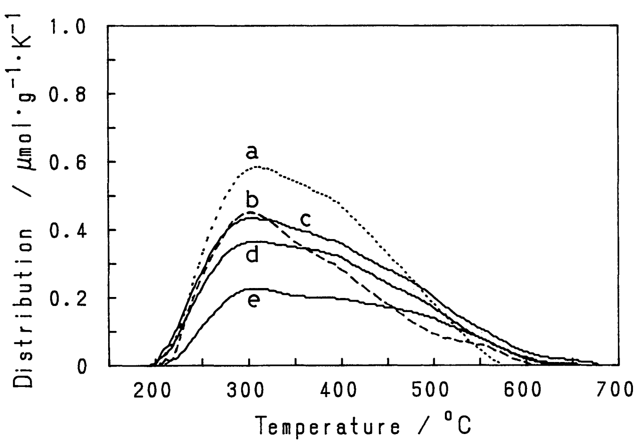

Fig. 6. TPD profiles of 2,6-dimethylpyridine. a, Original silica–alumina support (dotted line); b, CVD catalyst (dashed line): silica loading, 0.10; c, 0.20; d, 0.30; e, 0.39 g/g-support.

Table 1. Amounts of Pyridine and 2,6-Dimethylpyridine Desorbed from Catalysts

Catalyst (loading)a)	Adsorbate	Amount μmol/g-support		
		Total	400—500b)	>500b)
Support	Pyridine	190	44	35
(0)	2,6-DMP	126	33	7
CVD	Pyridine	102	18	12
(0.11)	2,6-DMP	84	17	5
CVD	Pyridine	130	28	25
(0.20)	2,6-DMP	108	29	13
CVD	Pyridine	99	30	17
(0.30)	2,6-DMP	84	26	10
CVD	Pyridine	62	14	11
(0.39)	2,6-DMP	58	17	10

a) Silica loading (g/g-support). b) Desorption temperature (°C).

temperature region, but increased in the high-temperature region, as can be understood from a comparison of curves d and b. This indicates that strong Brϕnsted acid sites, represented by the desorption of 2,6-DMP at temperatures above 500 °C, were increased together with a decrease in the total number of Brϕnsted acid sites.

Figure 6 illustrates the changes in the Brϕnsted acidity, measured by the desorption of 2,6-DMP, with a variation of silica loading; Table 1 summarizes the amounts of disorbed pyridine and 2,6-DMP. A small silica loading of 0.11 g/g-support decreased the total amounts of desorbed pyridine and 2,6-DMP. Interestingly, a further silica loading increased the total amounts, and enhanced the Brϕnsted acid strength. Especially, the number of strong Brϕnsted acid sites (expressed by the desorption of 2,6-DMP at temperatures above 400 °C) was maximized at silica loadings near 0.20 g/g-support. Above this loading, the total numbers of desorbed pyridine and 2,6-DMP monotonically decreased with increasing the silica loading. Another catalyst, such as a K^+ ion-exchanged silica–alumina, which gave no desorption of 2,6-DMP in the temperature region above 400 °C, exhibited no catalytic activity for 1-butene isomerization.14) The effective Brϕnsted acid sites for 1-butene isomerization held 2,6-DMP, even at high temperatures above 400 °C. The present TPD results indicate that strong Brϕnsted acid sites were generated upon depositing silica onto strong Lewis acid sites.

Catalytic Activities. The catalytic activities were examined for CVD catalysts prepared at 160 °C. Figure 7 shows the change in the cumene-cracking activity with process time at 350 °C. Cumene conversion was significantly improved by depositing silica on the

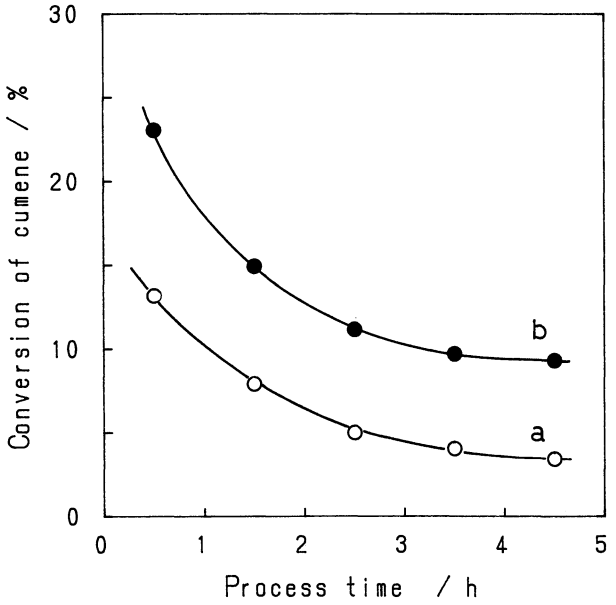

Fig. 7. Cumene conversion with process time. a, Original silica–alumina support; b, CVD catalyst (silica loading, 0.20 g/g-support).

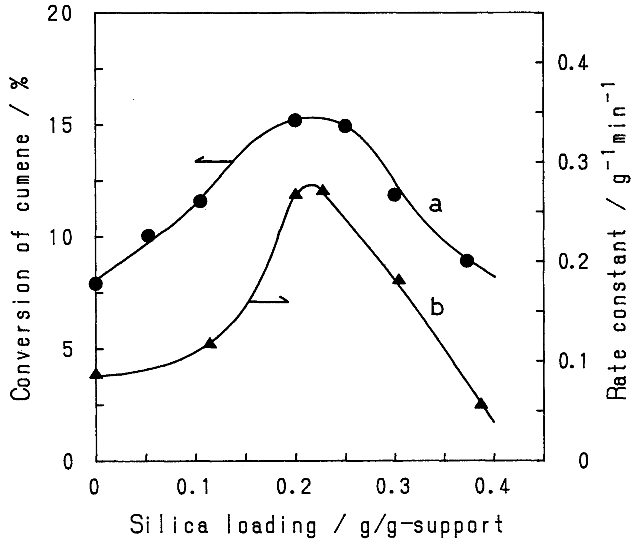

Fig. 8. Changes in the catalytic activities with silica loading. a, Cumene cracking at 350 °C; b, 1-butene isomerization at 50 °C.

original silica–alumina support. Figure 8 depicts the change in the catalytic activity for the cracking of cumene with silica loading, together with the results concerning the isomerization of 1-butene at 50 °C. Since the conversion of cumene decreased with the process time, the cracking activity was evaluated in terms of the average conversion during process times of 1—2 h. Cumene conversion increased with increasing silica loading, and attained a maximum at a silica loading of about 0.2 g/g-support. Above this loading, the cracking activity decreased with silica loading. For 1-butene isomerization, the initial first-order rate constant exhibited a maximum at a silica loading of about 0.2 g/g-support. This activity-pattern was similar to that for cumene conversion. Although the original silica–alumina support has essential activities for the reactions, the deposition of silica made it possible to increase the catalytic activities to twice the value for cumene cracking, and three times that for 1-butene isomerization, compared with the activity levels of the original silica–alumina support. In addition, with regard to the product distribution of 1-butene isomerization, the ratio of *cis-*/*trans-*2-butene was slightly decreased (from 0.95 to 0.83) with an increase in the silica loading, compared to the values at 1-butene conversion of 50%.

It is worth noting that the silica loading of a 0.2 g/g-support, at which catalytic activities were maximized, is equal to the loading at which the rate of silica deposition decelerated (Fig. 1), the loading at which the strong Brφnsted acid sites were maximized (Fig. 6 and Table 1), and the loading at which the surface area steeply decreased (Fig. 2). Below this critical loading, the catalytic activity for 1-butene isomerization was apparently unchanged (Fig. 8b). For the cracking of cumene, however, the cumene conversion increased with increasing silica loading (Fig. 8a). Since the pretreatment conditions for the cracking of cumene were different from those for the isomerization of 1-butene, the surface acidities are presumed to be different from each other. On the other hand, above the critical loading, the decreasing features in both the deposition rate and the catalytic activities are in fair agreement with the decreasing pattern in strong Brφnsted acidity of the CVD silica–alumina catalyst.

In view of practical usage, the present CVD catalyst was compared with an alumina-supported silica catalyst that has been previously reported.[9,14] For the isomerization of 1-butene, the alumina-supported silica catalyst was active, even at a low temperature of 0 °C,[14] and superior to the present CVD catalyst. This shows no discrepancy with the fact reported by Imizu and Tada.[8] In contrast, for the cracking of cumene, the present CVD silica–alumina catalyst was much preferable because even the original support was superior to the alumina-supported silica catalyst.[9] It is interesting that the enhanced activities vary regarding reaction type.

Formation of Active Site on Silica–Alumina Surface. Although the original silica–alumina support, itself, has Brφnsted acidity, an optimal silica deposit results in an increase in the number of strong Brφnsted acid sites as well as enhancements in catalytic activity. The superiority of CVD catalysts for catalytic reactions is presumably caused by an increase in the number of Brφnsted acid sites for CVD catalysts. When alumina is used as a support, these features are much clearer.[5,9,14] Since an alumina surface almost comprises Lewis acid sites, Brφnsted acid sites are effectively generated by the deposition of silica. The resulting alumina-supported silica shows significant catalytic activities for various reactions, whereas the alumina support showed few activities by itself. An excess of the silica deposit, however, weakened strong Brφnsted acid sites.[14]

The present silica–alumina support originally had not only strong Brφnsted acid sites, but also Lewis acid sites.[9] A small amount of silica loading decreased the number of strong Brφnsted acid sites (Fig. 6b). Prior to CVD operation, a support was heated at a low temperature of 160 °C in a stream of carrier gas, so that strong Lewis acid sites could be hydrated to form hydroxyl groups. Silica deposits proceed via an ester exchange of tetraethoxysilane with the surface hydroxyl groups. During the initial stage of deposition, a silica deposit is mainly initiated on strong Brφnsted acid sites, and contributes to a weakening of the acid strength. After the original Brφnsted acid sites are weakened, further silica deposition induces a transformation of Lewis acid sites into Brφnsted acid sites. Furthermore, an excess of silica deposits weaken Brφnsted acid sites. Consequently, strong Brφnsted acid sites were maximized at silica loadings close to 0.2 g/g-support, as shown in Table 1. Such Lewis acid sites are probably localized not on isolated alumina in the original silica–alumina, but on the boundary between silica and alumina. If Lewis acid sites exist on isolated alumina, the *cis*/*trans* ratio of produced 2-butene for 1-butene isomerization should be increased from 1 to close to about 3, which has been reported for silica overlayers deposited on alumina.[8] The ratio actually decreased to less than 1 for the present CVD silica–alumina. The difference in Lewis acidity of support materials results in variations of the catalytic properties for the above-mentioned reactions.

In conclusion, an enhancement of catalytic efficiency was achieved by depositing silica onto amorphous silica–alumina. This favorable nature should be attributed to an additional formaton of Brϕnsted acid sites which are ascribable to the transformation of Lewis acid sites through the CVD process.

References

1) M. Niwa, S. Kato, T. Hattori, and Y. Murakami, *J. Chem. Soc., Faraday Trans. 1*, **80**, 3135 (1984).

2) S. Sato, K. Urabe, and Y. Izumi, *J. Catal.*, **102**, 99 (1986).

3) S. Sato, S. Hasebe, H. Sakurai, K. Urabe, and Y. Izumi, *Appl. Catal.*, **29**, 107 (1987).

4) T. Okuhara and J. M. White, *Appl. Surf. Sci.*, **29**, 223 (1987).

5) S. Sato, M. Toita, Y. Q. Yu, T. Sodesawa, and F. Nozaki, *Chem. Lett.*, **1987**, 1535.

6) Y. Imizu, A. Tada, and I. Toyoshima, *Shokubai* (*Catalyst*), **30**, 388 (1988).

7) M. Niwa, T. Hibino, H. Murata, N. Katada, and Y. Murakami, *J. Chem. Soc., Chem. Commun.*, **1989**, 289.

8) Y. Imizu and A. Tada, *Chem. Lett.*, **1989**, 1793.

9) S. Sato, M. Toita, T. Sodesawa, and F. Nozaki, *Appl. Catal.*, **62**, 73 (1990).

10) R. W. Cranston and F. A. Inkley, *Adv. Catal.*, **9**, 143 (1957).

11) B. C. Lippens, B. G. Linsen, and J. H. de Boer, *J. Catal.*, **3**, 32 (1964).

12) B. C. Lippens and J. H. de Boer, *J. Catal.*, **4**, 319 (1965).

13) J. H. de Boer, B. G. Linsen, Th. van der Plas, and G. J. Zondervan, *J. Catal.*, **4**, 649 (1965).

14) S. Sato, M. Tokumitsu, T. Sodesawa, and F. Nozaki, *Bull. Chem. Soc. Jpn.*, **64**, 1005 (1991).

15) H. A. Benesi, *J. Catal.*, **28**, 176 (1973).

16) A. Corma, C. Rodellas, and V. Fornes, *J. Catal.*, **88**, 374 (1984).

17) L. L. Murrell and N. C. Dispenziere, Jr., *J. Catal.*, **117**, 275 (1989).